

Spatiotemporal Characterization of Active Brownian Dynamics in Channels

Yanis Baouche,^{1,*} Mathis Guéneau,^{1,*} and Christina Kurzthaler^{1,2,3,†}

¹*Max-Planck-Institut für Physik komplexer Systeme, Nöthnitzer Straße 38, 01187 Dresden, Germany*

²*Center for Systems Biology Dresden, Pfotenhauerstraße 108, 01307 Dresden, Germany*

³*Cluster of Excellence, Physics of Life, TU Dresden, Arnoldstraße 18, 01062 Dresden, Germany*

Accumulation at boundaries represents a widely observed phenomenon in active systems with implications for microbial ecology and engineering applications. To rationalize the underlying physics, we provide analytical predictions for the first-passage properties and spatial distributions of a confined active Brownian particle (ABP). We show that ABPs with absorbing and hard-wall boundary conditions are Siegmund duals, yielding a direct mapping between the propagators of the two problems. We analyze the system across low and high activity regimes – quantifying persistent motion relative to diffusion – and show that active motion, together with a favorable initial orientation, typically lowers the mean first-passage time relative to passive diffusion. Notably, the full time-dependent propagator between hard walls approaches a wall-accumulated stationary state given by the derivative of the splitting probability as a consequence of Siegmund duality.

Active agents inevitably engage with boundaries: not only do the latter facilitate foraging and survival of microorganisms via surface-concentrated nutrients and biofilm formation, they also mediate their navigation by enabling persistent exploration in the absence of complex sensing behavior [1–8]. Boundaries are also the pivot point for functional tasks, where future microrobots are expected to translate their energy into mechanical work for performing therapeutic or engineering operations [9–14]. To guide the design of these applications and obtain a physical understanding of the microbiological phenomena, it is crucial to unravel two questions: first, how long does it take an active agent to reach a boundary and, second, how do boundaries alter their distributions.

To address these topics, a number of models – including the canonical active Brownian particle (ABP) [15–22], the active Ornstein–Uhlenbeck particle [23], and the run-and-tumble particle [24–30] – have shown how the intrinsic dynamics leverage activity to enable accelerated

target reaching in comparison to passive particles. Confined dynamics also display characteristic phenomena: highly-active particles can accumulate near walls [31, 32] without the need of hydrodynamics, while the time it takes agents to escape a wide, slowly varying channel has been linked to their distribution near the boundaries [33], reflecting the curvature-dependent pressure field of active systems [34–36]. The phenomenology of boundary interactions is thus rich, yet the coupling between translational and rotational degrees of freedom makes deriving analytical expressions for confined active dynamics challenging and requires new theoretical frameworks.

A particularly useful tool is Siegmund duality [37, 38], which establishes an exact correspondence between stochastic dynamics with absorbing and hard boundaries (Fig. 1). Specifically, for two walls separated by L , the hard-wall propagator $p_H(z, t|z_0)$ (i.e., the probability density to be at position z at time t , given initial position z_0), follows from the absorbing-wall propagator p_A via:

$$p_H(z, t|z_0) = \int_{z_0}^L dz' \frac{\partial}{\partial z} p_A(z', t|z). \quad (1)$$

A similar relation can be derived to compute p_A from p_H ; thus the solution for one boundary condition (BC) determines the solution for the other.

Siegmund duality, first noted for Brownian motion [39, 40] and later formalized in [37], constitutes a particular instance of a Markov duality [41–43]. At its core lies a time-reversal symmetry relating the forward generator of a process to the backward generator of its dual [38]. Constructing the dual of a stochastic process is, however, generally a nontrivial task. Only recently explicit constructions have been obtained for a broad class of stochastic processes, including active particles [38, 44–46]. Here, we first show that ABPs confined between absorbing and hard walls form a Siegmund-dual pair. Then, we derive a systematic expansion in the low-activity regime for the absorbing-wall propagator and analyze the high-activity regime in the long-time limit, providing access to the

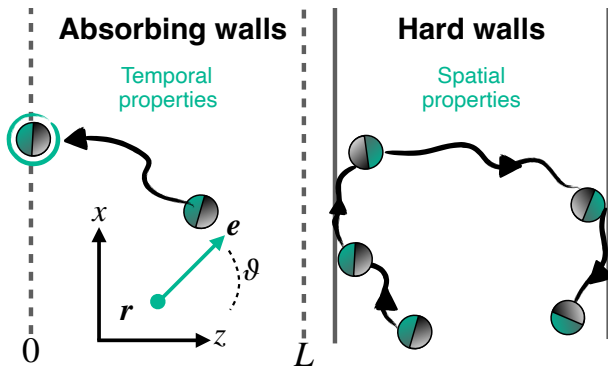


Figure 1. Schematic of the duals: ABPs between absorbing (sticking) and hard (reflective) walls. The left side shows an ABP hitting an absorbing boundary, which gives access to first-passage properties. The right side illustrates the dynamics between hard walls, yielding particle distributions. The inset depicts the agent’s position r and orientation ϑ .

first-passage statistics and serving as input for Eq. (1). Our analytical results show that, depending on the initial position and orientation, activity can either enhance or hinder time efficiency. Moreover, the dynamics between hard-walls relaxes to a wall-accumulated stationary state, akin to that found in many active systems [8, 32, 47–49].

Model.— We consider the motion of a two-dimensional ABP moving at a constant speed v along its instantaneous orientation $\mathbf{e}(t) = (\cos \vartheta(t), \sin \vartheta(t))$, which is subject to rotational diffusion with diffusivity D_{rot} . The particle position also experiences translational diffusion with diffusivity D . The position $\mathbf{r}(t) = (x(t), z(t))$ and orientation $\vartheta(t)$ are governed by the Langevin equations:

$$\dot{\mathbf{r}} = v\mathbf{e} + \sqrt{2D}\boldsymbol{\eta} \quad \text{and} \quad \dot{\vartheta} = \sqrt{2D_{\text{rot}}}\xi, \quad (2)$$

where $\boldsymbol{\eta}(t)$ and $\xi(t)$ are independent, delta-correlated Gaussian white noises with zero mean. The ABP is confined between two walls located at $z = 0$ and $z = L > 0$ with two different BCs: *absorbing* (A) and *hard* (H) *walls*. Its dynamics are characterized by three timescales: the diffusive time $\tau = L^2/D$, the ballistic time $\tau_a = L/v$, and the rotational diffusion time $\tau_{\text{rot}} = 1/D_{\text{rot}}$. This entails two nondimensional numbers: the Péclet number $\text{Pe} = \tau/\tau_a$, measuring active motion relative to diffusion, and $\gamma = \tau/\tau_{\text{rot}}$, reflecting the importance of translational *vs.* rotational diffusion.

Since we are only interested in the dynamics perpendicular to the walls, we focus on the z -coordinate. We denote the associated propagators, averaged over the equilibrium initial orientation, i.e. $p_{\text{eq}}(\vartheta_0) = 1/(2\pi)$, and integrated over the final orientation, by

$$p_{A,H}(z, t | z_0) = \int d\vartheta \int \frac{d\vartheta_0}{2\pi} p_{A,H}(z, \vartheta, t | z_0, \vartheta_0), \quad (3)$$

where $p_{A,H}(z, \vartheta, t | z_0, \vartheta_0) dz d\vartheta$ is the probability that the ABP is found in the interval $[z, z + dz]$ with orientation in $[\vartheta, \vartheta + d\vartheta]$ at time t , given the initial conditions $z(t = 0) = z_0$ and $\vartheta(t = 0) = \vartheta_0$. To demonstrate Eq. (1), we adapt the main steps of Ref. [38] for our set-up.

Absorbing (sticking) walls.— We first consider an ABP with sticking absorption at $z = 0$ and $z = L$: upon first hitting either wall, the particle remains there for all later times. Accordingly, the propagator may contain Dirac masses at $z = 0$ and $z = L$ weighted by the time-integrated incoming boundary flux up to time t . It satisfies the backward Fokker–Planck equation (FPE)

$$\partial_t p_A(z, t | z_0, \vartheta_0) = \mathcal{L}_{z_0, \vartheta_0}^\dagger p_A(z, t | z_0, \vartheta_0), \quad (4a)$$

$$\mathcal{L}_{z_0, \vartheta_0}^\dagger := v \cos \vartheta_0 \partial_{z_0} + D \partial_{z_0}^2 + D_{\text{rot}} \partial_{\vartheta_0}^2, \quad (4b)$$

where the backward generator $\mathcal{L}_{z_0, \vartheta_0}^\dagger$ acts on the *initial* variables (z_0, ϑ_0) , and we have averaged over the final orientation. We define the probability to find the ABP

in $[\ell_A > 0, L]$ at time t with initial conditions (z_0, ϑ_0) :

$$Q_A(\ell_A, t | z_0, \vartheta_0) := \mathbb{P}_A(z(t) \geq \ell_A | z_0, \vartheta_0), \quad (5a)$$

$$= \int_{\ell_A}^L dz p_A(z, t | z_0, \vartheta_0). \quad (5b)$$

Since \mathcal{L}^\dagger acts only on the initial variables, integrating Eq. (4a) over $z \in [\ell_A, L]$ yields

$$\partial_t Q_A(\ell_A, t | z_0, \vartheta_0) = \mathcal{L}_{z_0, \vartheta_0}^\dagger Q_A(\ell_A, t | z_0, \vartheta_0), \quad (6)$$

subject to BCs $Q_A(\ell_A, t | 0, \vartheta_0) = 0$, since a particle started at $z = 0$ is absorbed immediately, and $Q_A(\ell_A, t | L, \vartheta_0) = 1$, as a particle starting at $z = L$ is absorbed and $z = L \geq \ell_A$. Moreover, the initial condition $Q_A(\ell_A, 0 | z_0, \vartheta_0) = \mathbf{1}_{\{z_0 \geq \ell_A\}}$ follows from $p_A(z, 0 | z_0, \vartheta_0) = \delta(z - z_0)$.

Hard (reflective) walls.— We next consider an ABP between two hard walls at $z = 0$ and $z = L$ and denote by $p_H(z, \vartheta, t | \tilde{z}_0)$ the probability density averaged over the initial angle. It satisfies the forward FPE

$$\partial_t p_H(z, \vartheta, t | \tilde{z}_0) = \mathcal{L}_{z, \vartheta} p_H(z, \vartheta, t | \tilde{z}_0), \quad (7a)$$

$$\mathcal{L}_{z, \vartheta} := -v \cos \vartheta \partial_z + D \partial_z^2 + D_{\text{rot}} \partial_\vartheta^2, \quad (7b)$$

where the forward generator $\mathcal{L}_{z, \vartheta}$ acts on the *final* variables (z, ϑ) . The system is subject to no-flux BCs: $v \cos \vartheta p_H - D \partial_z p_H = 0$ at $z = 0$ and L . We now define the conditional probability to find the ABP in $[0, \ell_H]$ at time t given the fixed final orientation $\vartheta(t) = \vartheta$ as

$$Q_H(\ell_H, t | \vartheta, \tilde{z}_0) := \mathbb{P}_H(z(t) \leq \ell_H | \vartheta, \tilde{z}_0), \quad (8a)$$

$$= \frac{\int_0^{\ell_H} dz p_H(z, \vartheta, t | \tilde{z}_0)}{p_{\text{eq}}(\vartheta)}. \quad (8b)$$

Here, Eq. (8b) follows from Bayes' rule: $p_H(z, t | \vartheta, \tilde{z}_0) = p_H(z, \vartheta, t | \tilde{z}_0)/p(\vartheta, t | \tilde{z}_0)$. As $\vartheta(t)$ evolves independently of $z(t)$ and is initialized at stationarity, $\vartheta(0) \sim p_{\text{eq}}(\vartheta)$, its marginal remains $p_{\text{eq}}(\vartheta)$ for all t (hence $p(\vartheta, t | \tilde{z}_0) = p_{\text{eq}}(\vartheta)$). Further, since $p_{\text{eq}}(\vartheta) = 1/(2\pi)$ is ϑ -independent, integrating Eq. (7a) over $z \in [0, \ell_H]$ yields [50]

$$\partial_t Q_H(\ell_H, t | \vartheta, \tilde{z}_0) = \mathcal{L}_{\ell_H, \vartheta} Q_H(\ell_H, t | \vartheta, \tilde{z}_0). \quad (9)$$

Translational Brownian noise prevents singular boundary masses. Therefore, the probability to lie in $[0, \ell_H]$ vanishes at $\ell_H = 0$, yielding the BC $Q_H(0, t | \vartheta, \tilde{z}_0) = 0$. Further, hard-wall confinement enforces $z(t) \in [0, L]$ for all t , hence $Q_H(L, t | \vartheta, \tilde{z}_0) = 1$, and the localized start $p_H(z, \vartheta, 0 | \tilde{z}_0) = \delta(z - \tilde{z}_0)$ translates to $Q_H(\ell_H, 0 | \vartheta, \tilde{z}_0) = \mathbf{1}_{\{\ell_H \geq \tilde{z}_0\}}$.

Siegmund duality.— Under the angle shift $\vartheta = \vartheta_0 + \pi$, the generators given in Eqs. (4b) and (7b) match $\mathcal{L}_{z_0, \vartheta_0 + \pi} = \mathcal{L}_{z_0, \vartheta_0}^\dagger$, i.e., the hard-wall process at time t is conditioned on an orientation opposite to the absorbing process's initial one. Identifying $\ell_A = \tilde{z}_0$ in Eq. (5a)

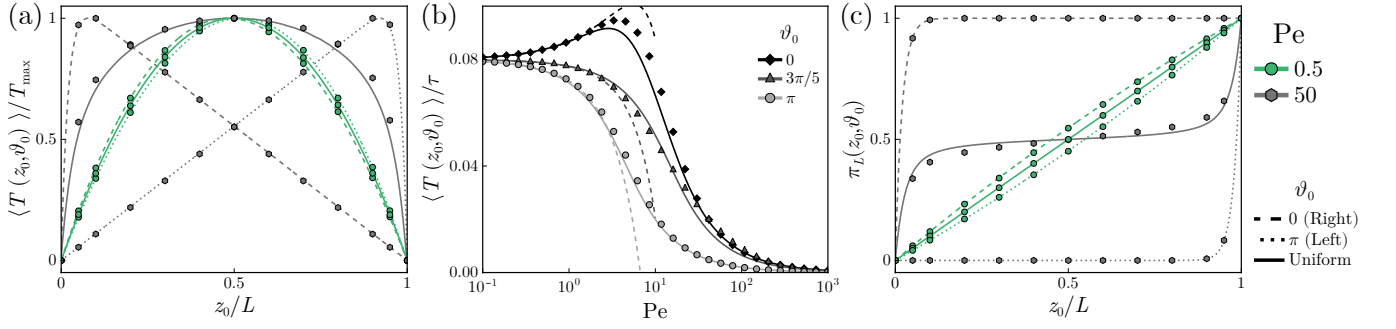


Figure 2. First-passage properties. (a) Mean-first-passage time $\langle T \rangle$ normalized by its maximum T_{\max} , as a function of the initial position z_0 . (b) Mean-first-passage time $\langle T \rangle$ as a function of the Péclet number and for $z_0/L = 0.2$. (c) Splitting probability π_L at the right wall as a function of z_0 . In (a–c) we set $\gamma = 3$. In (b), dashed and solid lines denote the low- Pe expansion up to $O(Pe^2)$ and the high-activity result [Eq. (16)], respectively. Symbols correspond to simulation results.

and $\ell_H = z_0$ in Eq. (8a), their initial conditions also coincide. Given these constraints, $Q_H(z_0, t | \vartheta(t) = \vartheta_0 + \pi, \tilde{z}_0)$ and $Q_A(\tilde{z}_0, t | z_0, \vartheta_0)$ satisfy the same differential equation with the same boundary and initial conditions, and are therefore equal. Averaging over $\vartheta_0 \sim p_{\text{eq}}$ and using the invariance of p_{eq} under $\vartheta_0 \mapsto \vartheta_0 + \pi$ yields the ABP Siegmund duality relation [37, 38]

$$\mathbb{P}_H(z(t) \leq z_0 | \tilde{z}_0) = \mathbb{P}_A(z(t) \geq \tilde{z}_0 | z_0). \quad (10)$$

Hence, after averaging the initial orientations over $p_{\text{eq}}(\vartheta)$, the probability that the hard-wall ABP started at \tilde{z}_0 lies to the left of z_0 at time t equals the probability that the absorbing ABP started at z_0 lies to the right of \tilde{z}_0 at the same time. Differentiating Eq. (10) with respect to z_0 , and renaming variables, straightforwardly gives the announced result in Eq. (1).

The duality relation [Eq. (10)] also allows deriving the survival probability from the hard-wall propagator via

$$S(z_0, t) = \int_0^{z_0} dz [p_H(z, t|0) - p_H(z, t|L)], \quad (11)$$

and relates the mean-first-passage time (MFPT) from z_0 to either wall to the local time spent by ABPs in $[0, z_0]$ between hard walls (see End Matter):

$$\langle T \rangle = \int_0^{z_0} dz \int_0^\infty dt [p_H(z, t|0) - p_H(z, t|L)]. \quad (12)$$

First-passage properties.— We decompose the propagator of an ABP between absorbing walls $p_A(z, t|z_0)$ as

$$p_A = P_A + E_0 \delta(z) + E_L \delta(z - L), \quad (13)$$

where $P_A(z, t|z_0)$ denotes the probability density of an ABP between absorbing (non-sticking) walls (i.e. $P_A(z = 0, t) = P_A(z = L, t) = 0$) and boundary masses are encoded in the exit probabilities:

$$E_{0,L}(z_0, t) = \pm D \int_0^t dt' \partial_z P_A(z, t'|z_0)|_{z=0,L}. \quad (14)$$

In the low activity regime ($Pe \ll 1$), where translational diffusion dominates over active motion, we compute $P_A(z, t|z_0) = \int d\vartheta \int d\vartheta_0 P_A(z, \vartheta, t|\vartheta_0, z_0)/(2\pi)$ by solving the forward FPE [Eq. (7a)] with initial condition $P_A(z, \vartheta, t = 0|\vartheta_0, z_0) = \delta(z - z_0)\delta(\vartheta - \vartheta_0)$. The time-dependent behavior can be obtained by first moving to Laplace space ($t \mapsto s$) and inserting the Péclet number expansion $P_A = \hat{P}_A^{(0)} + Pe \hat{P}_A^{(1)} + Pe^2 \hat{P}_A^{(2)} + O(Pe^3)$ into Eq. (7a). Here, $\hat{P}_A^{(0)}$ corresponds to the propagator of a diffusive particle (with rotational diffusion) between two absorbing walls and can be readily computed using the method of reflections (see End Matter). This procedure yields a recursive relation

$$\begin{aligned} \hat{P}_A^{(i+1)}(z, \vartheta, s|z_0, \vartheta_0) &= \int_0^L dz' \int_0^{2\pi} d\vartheta' \hat{P}_A^{(0)}(z, \vartheta, s|z', \vartheta') \\ &\times \left[-(D/L) \cos(\vartheta') \partial_{z'} \hat{P}_A^{(i)}(z', \vartheta', s|z_0, \vartheta_0) \right]. \end{aligned} \quad (15)$$

We then use the survival probability $\hat{S}(s|z_0, \vartheta_0) = \int_0^{2\pi} \int_0^L \hat{P}_A(z, \vartheta, s|z_0, \vartheta_0) dz d\vartheta$ to compute the MFPT via $\langle T \rangle = \hat{S}(s = 0|z_0, \vartheta_0)$ [Fig. 2].

Analytical progress is also possible in the high-activity regime, where persistent motion dominates over orientational diffusion $\tau_a \ll \tau_{\text{rot}}$ (i.e., $\gamma \ll Pe$). Therefore, we introduce $\epsilon = \gamma/Pe$ and first look into the boundary layer of width $O(\epsilon)$. Rescaling the equation for the MFPT, $\mathcal{L}_{z_0, \vartheta_0}^\dagger \langle T \rangle = -1$, with the stretched coordinate $y = (z_0 - L)/(L\epsilon)$ shows that (close to the walls) rotational diffusion can be neglected, given $\gamma \ll Pe^{2/3}$. Neglecting rotational diffusion and taking the BCs $\langle T(0, \vartheta_0) \rangle = \langle T(L, \vartheta_0) \rangle = 0$, we obtain (for $\cos \vartheta_0 \neq 0$):

$$\langle T \rangle_{\gamma/Pe \rightarrow 0} = \frac{\tau}{Pe \cos \vartheta_0} \left[\frac{1 - e^{-Pe \cos(\vartheta_0) z_0/L}}{1 - e^{-Pe \cos(\vartheta_0)}} - \frac{z_0}{L} \right] \quad (16)$$

Our results [Fig. 2(a)] show that randomly-oriented, active particles take the longest when starting at the channel's midpoint, with a symmetric MFPT w.r.t. the initial position z_0 . This picture changes for particles initially

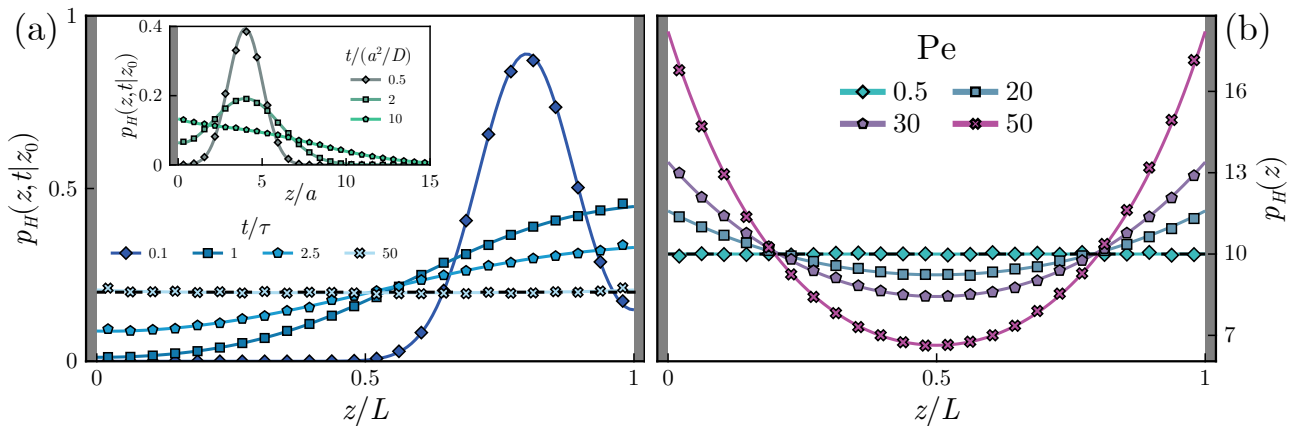


Figure 3. Probability densities of an ABP between hard walls. (a) Probability density $p_H(z, t|z_0)$ as a function of the position z for different times t . Here, $z_0/L = 0.8$ and $Pe = 0.5$. Lines correspond to the low-Pe (up to $O(Pe^2)$) expansion and symbols are simulation results. (*Inset*) Probability density $p_H(z, t|z_0)$ for the case of a single wall at $z = 0$. We set $z_0/a = 4$ and $Pe = 0.5$, and rescale length scales with the particle's hydrodynamic radius $a = \sqrt{3D/(4D_{\text{rot}})}$. (b) Stationary distribution $p_H(z)$ for different Péclet numbers. Lines correspond to the high-Pe solution (18) and symbols are simulation results. (a–b) Vertical gray lines indicate the walls.

oriented towards the right wall ($z_0/L = 1$): At low activity ($Pe = 0.5$), the maximal MFPT shifts to $z_0/L \lesssim 0.5$ and becomes asymmetric, because active motion helps the particle to reach the right wall (towards which it is oriented) faster. For large Péclet numbers ($Pe = 50$), the peak of the MFPT shifts towards $z_0 \gtrsim 0$ and decays linearly thereafter, which reflects the typical time taken by a persistent particle to cover the remaining distance at constant speed: $\langle T \rangle \simeq (L - z_0)/v$. The picture reverses when the particle initially travels towards the left wall.

To investigate the impact of translational-rotational coupling on the MFPT, we consider its behavior as a function of the Péclet number [Fig. 2(b)]. Interestingly, the MFPT exhibits a non-monotonic behavior, for particles starting close to a wall and departing towards the opposite one. While the agent could still reach the closer boundary through diffusion at low activity ($Pe \simeq 1$), it reaches the opposite boundary almost instantaneously for $Pe \gtrsim 100$. In between lies the regime of moderate activity where rotational diffusion could kick in and reorient it, thus slowing it down. The latter happens when active and reorientation time scales are comparable, i.e. when $\tau_a/\tau_{\text{rot}} = \gamma/Pe = O(1)$. In addition, we note that the low-Pe solution can still properly capture the maximum around $Pe \simeq 10$ but becomes unreliable after that. The high-activity solution also gives a very good agreement at moderate and low Pe, as it interpolates to the Brownian solution $\langle T \rangle = z_0(L - z_0)/(2D)$ for $Pe \rightarrow 0$ [Eq. (16)].

Another important first-passage quantity is the splitting probability [51–53], i.e., the probability that the agent reaches the right wall before the left one. For small Pe, it can be computed as the long-time limit of the exit probability $\pi_L(z_0) = E_L(z_0, t \rightarrow \infty)$ [Eq. (14)]. For high activity, we employ the same approach as for $\langle T \rangle$

(with BCs $\pi_L(0, \vartheta_0) = 0$, $\pi_L(L, \vartheta_0) = 1$), leading to:

$$\pi_L(z_0, \vartheta_0) \underset{\gamma/Pe \rightarrow 0}{=} \frac{1 - e^{-Pe \cos(\vartheta_0) z_0/L}}{1 - e^{-Pe \cos(\vartheta_0)}}. \quad (17)$$

For randomly-oriented agents, the splitting probability at the right wall π_L increases almost linearly with z_0 at low activity, where translational diffusion dominates [Fig. 2(c)]. Our results further show that particles initially oriented towards the right wall have a higher probability of reaching it than those oriented away from it. The difference in probabilities becomes smaller at the boundaries, where translational diffusion outperforms active motion. At high activity, however, π_L approaches a plateau at ≈ 0.5 for most z_0 , reflecting the ballistic motion of the particle towards either wall with equal probability. For a fixed initial orientation, the behavior drastically changes: π_L jumps to 1 when ϑ_0 points towards the wall at $z = L$, and to 0 when it points towards the opposite one.

Confined particles.— Leveraging Siegmund's duality [Eq. (1)] and Eq. (15), we compute the time-dependent propagator in the presence of hard-walls $p_H(z, t|z_0)$. Setting $\tilde{z}_0 = L$ in Eq. (10) and taking $t \rightarrow \infty$ shows that the stationary distribution $p_H(z) = p_H(z, t \rightarrow \infty|z_0)$ is a simple derivative of the splitting probability [38, 44] (see End Matter). In the high-activity regime, it can be thus computed from Eq. (17) and reads

$$p_H(z) = \frac{\partial \pi_L}{\partial z} = \frac{Pe}{2\pi L} \int_0^{2\pi} \cos(\vartheta_0) \frac{e^{-Pe \cos(\vartheta_0) z/L}}{1 - e^{-Pe \cos(\vartheta_0)}} d\vartheta_0, \quad (18)$$

see also [32]. Figure 3 (a) shows how, starting from a localized initial condition, the probability density spreads over the channel width and eventually reaches a stationary distribution. The latter evolves from an almost uni-

form profile at low activity ($Pe = 0.5$) to an increasingly pronounced U-shaped profile as activity increases [Fig. 3(b)], indicating enhanced wall accumulation. In our model, this accumulation results solely from the interactions of active agents with hard walls, as active particles remain near the boundary until rotational diffusion allows them to reorient and escape. This finding is in qualitative agreement with experimental [47–49] and computational [32] observations, yet the importance of steric *vs.* hydrodynamic interactions [49], yielding similar wall-accumulated distributions, may depend on the specific systems.

The time-dependent propagator with hard walls (in the low- Pe regime) provides direct access to the moments of the position $\langle z^n(t) \rangle = \int_0^L p_H(z, t|z_0) z^n dz$. As suggested from the stationary probability, the mean position converges to the channel’s midpoint, $\langle z(t) \rangle_{t \rightarrow \infty} = L/2$, while the fluctuations around it are perturbed $\langle (z(t) - \langle z(t) \rangle)^2 \rangle_{t \rightarrow \infty} = (L^2/12) + APe^2 + O(Pe^4)$ with $A > 0$, showing that activity enhances the uniform Brownian result.

Finally, our model recovers the one-wall problem in the limit of infinite channel width, $L \rightarrow \infty$ [Fig. 3(a)(inset)]. In this case, the MFPT diverges [16] and no stationary distribution exists: without the right boundary, the particle can escape to infinity, leading to a probability density that broadens continuously in space over time.

Conclusions. – We formally showed that ABPs moving between hard and absorbing boundaries are Siegmund duals, allowing analytical predictions for one problem to be obtained from the other. In particular, a systematic low-Péclet expansion derived for the absorbing problem can be transferred through the duality to the time-dependent probability density between hard walls. We thereby characterized the evolution towards a stationary wall-accumulated state, thus providing a theoretical footing for experimental and computational observations of active agents. Our work completes our understanding of active Brownian transport in channels, by unraveling how the interplay of active motion and diffusion dictates first-passage statistics of active agents between two walls.

The formalism employed here offers a systematic approach for accessing both time-related efficiencies and spatial distribution properties, in a class of problems that are otherwise difficult to address. It admits several extensions: these include alternative agent dynamics, such as run-and-tumble motion [44, 54–57], stochastic resetting processes [38, 58–61], non-Markovian processes [38, 62, 63], higher-dimensional settings, more complex geometries, e.g., structured [33, 64, 65] walls, and partially-absorbing boundaries [66–68]. The latter problems may prove more tractable in one setting – absorbing or reflecting – whose solution can be systematically transferred to its dual counterpart. This framework may thus enable progress in quantifying biological and soft-matter systems, where confinement strongly reg-

ulates transport and reaction efficiency, while systematic theoretical approaches remain comparatively scarce.

Acknowledgments. – M.G. thanks L. Touzo for insightful discussions on Siegmund duality and for past collaborations on this topic. We further thank Thomas Franosch for helpful discussions.

* contributed equally

† kurzthaler@pks.mpg.de

- [1] R. Di Leonardo, L. Angelani, D. Dell’Arciprete, G. Ruocco, V. Iebba, S. Schippa, M. P. Conte, F. Mecarini, F. De Angelis, and E. Di Fabrizio, Bacterial ratchet motors, *Proceedings of the National Academy of Sciences* **107**, 9541–9545 (2010).
- [2] D. Ray, C. Reichardt, and C. J. O. Reichardt, Casimir effect in active matter systems, *Physical Review E* **90**, 013019 (2014).
- [3] P. Galajda, J. Keymer, P. Chaikin, and R. Austin, A wall of funnels concentrates swimming bacteria, *Journal of Bacteriology* **189**, 8704–8707 (2007).
- [4] C. Bechinger, R. Di Leonardo, H. Löwen, C. Reichardt, G. Volpe, and G. Volpe, Active particles in complex and crowded environments, *Reviews of Modern Physics* **88**, 045006 (2016).
- [5] J. Simmchen, J. Katuri, W. E. Uspal, M. N. Popescu, M. Tasinkevych, and S. Sánchez, Topographical pathways guide chemical microswimmers, *Nature Communications* **7**, 10598 (2016).
- [6] G. C. L. Wong, J. D. Antani, P. P. Lele, J. Chen, B. Nan, M. J. Kühn, A. Persat, J.-L. Bru, N. M. Høyland-Kroghsbo, A. Siryaporn, J. C. Conrad, F. Carrara, Y. Yawata, R. Stocker, Y. V. Brun, G. B. Whitfield, C. K. Lee, J. d. Anda, W. C. Schmidt, R. Golestanian, G. A. O’Toole, K. A. Floyd, F. H. Yildiz, S. Yang, F. Jin, M. Toyofuku, L. Eberl, N. Nomura, L. A. Zacharoff, M. Y. El-Naggar, S. E. Yalcin, N. S. Malvankar, M. D. Rojas-Andrade, A. I. Hochbaum, J. Yan, H. A. Stone, N. S. Wingreen, B. L. Bassler, Y. Wu, H. Xu, K. Drescher, and J. Dunkel, Roadmap on emerging concepts in the physical biology of bacterial biofilms: from surface sensing to community formation, *Physical Biology* **18**, 051501 (2021).
- [7] O. Hallatschek, S. S. Datta, K. Drescher, J. Dunkel, J. Elgeti, B. Waclaw, and N. S. Wingreen, Proliferating active matter, *Nature Reviews Physics* **5**, 407–419 (2023).
- [8] P. Denissenko, V. Kantsler, D. J. Smith, and J. Kirkman-Brown, Human spermatozoa migration in microchannels reveals boundary-following navigation, *Proceedings of the National Academy of Sciences* **109**, 8007–8010 (2012).
- [9] G. Gompper, H. A. Stone, C. Kurzthaler, D. Saintillan, F. Peruani, D. A. Fedosov, T. Auth, C. Cottin-Bizonne, C. Ybert, E. Clément, T. Darnige, A. Lindner, R. E. Goldstein, B. Liebchen, J. Binysh, A. Souslov, L. Isa, R. di Leonardo, G. Frangipane, H. Gu, B. J. Nelson, F. Brauns, M. C. Marchetti, F. Cichos, V.-L. Heuthe, C. Bechinger, A. Korman, O. Feinerman, A. Cavagna, I. Giardina, H. Jeckel, and K. Drescher, The 2025 motile active matter roadmap, *Journal of Physics: Condensed*

- Matter* **37**, 143501 (2025).
- [10] V. A. Baulin, A. Giacometti, D. A. Fedosov, S. Ebbens, N. R. Varela-Rosales, N. Feliu, M. Chowdhury, M. Hu, R. Füchslin, M. Dijkstra, M. Mussel, R. v. Roij, D. Xie, V. Tzanov, M. Zu, S. Hidalgo-Caballero, Y. Yuan, L. Cocconi, C.-M. Ghim, C. Cottin-Bizonne, M. Carmen Miguel, M. Jose Esplandiú, J. Simmchen, W. J. Parak, M. Werner, G. Gompper, and M. M. Hanczyc, Intelligent soft matter: towards embodied intelligence, *Soft Matter* **21**, 4129–4145 (2025).
- [11] G. Volpe, N. A. M. Araújo, M. Guix, M. Miodownik, N. Martin, L. Alvarez, J. Simmchen, R. D. Leonardo, N. Pellicciotta, Q. Martinet, J. Palacci, W. K. Ng, D. Saxena, R. Sapienza, S. Nadine, J. F. Mano, R. Mahdavi, C. Beck Adiels, J. Forth, C. Santangelo, S. Palagi, J. M. Seok, V. A. Webster-Wood, S. Wang, L. Yao, A. Aghakhani, T. Barois, H. Kellay, C. Coulais, M. van Hecke, C. J. Pierce, T. Wang, B. Chong, D. I. Goldman, A. Reina, V. Trianni, G. Volpe, R. Beckett, S. P. Nair, and R. Armstrong, Roadmap for animate matter, *Journal of Physics: Condensed Matter* **37**, 333501 (2025).
- [12] P. Erkoç, I. C. Yasa, H. Ceylan, O. Yasa, Y. Alapan, and M. Sitti, Mobile Microrobots for Active Therapeutic Delivery, *Advanced Therapeutics* **2**, 1800064 (2019).
- [13] Y. Alapan, O. Yasa, B. Yigit, I. C. Yasa, P. Erkoç, and M. Sitti, Microrobotics and Microorganisms: Biohybrid Autonomous Cellular Robots, *Annual Review of Control, Robotics, and Autonomous Systems* **2**, 205 (2019).
- [14] R. Nauber, S. R. Goudu, M. Goeckenjan, M. Bornhäuser, C. Ribeiro, and M. Medina-Sánchez, Medical microrobots in reproductive medicine from the bench to the clinic, *Nature Communications* **14**, 728 (2023).
- [15] F. Di Trapani, T. Franosch, and M. Caraglio, Active Brownian particles in a circular disk with an absorbing boundary, *Physical Review E* **107**, 064123 (2023).
- [16] Y. Baouche, M. Le Goff, C. Kurzthaler, and T. Franosch, First-passage-time statistics of active Brownian particles: A perturbative approach, *Physical Review E* **111**, 054113 (2025).
- [17] S. A. Iyaniwura and Z. Peng, Mean first passage time of active Brownian particles in two dimensions, *New Journal of Physics* **27**, 104401 (2025).
- [18] U. Basu, S. N. Majumdar, A. Rosso, and G. Schehr, Active Brownian motion in two dimensions, *Physical Review E* **98**, 062121 (2018).
- [19] U. Basu, S. N. Majumdar, A. Rosso, and G. Schehr, Long-time position distribution of an active Brownian particle in two dimensions, *Physical Review E* **100**, 062116 (2019).
- [20] A. Poncet, O. Bénichou, V. Démercy, and D. Nishiguchi, Pair correlation of dilute active Brownian particles: From low-activity dipolar correction to high-activity algebraic depletion wings, *Physical Review E* **103**, 012605 (2021).
- [21] M. Caraglio, Two-dimensional active Brownian particles crossing a parabolic barrier: finite rectangular domain with absorbing boundary conditions, *Journal of Statistical Mechanics: Theory and Experiment* **2026**, 023205 (2026).
- [22] I. Santra, U. Basu, and S. Sabhapandit, Active brownian motion with directional reversals, *Physical Review E* **104**, L012601 (2021).
- [23] E. Woillez, Y. Kafri, and V. Lecomte, Nonlocal stationary probability distributions and escape rates for an active Ornstein–Uhlenbeck particle, *Journal of Statistical Mechanics: Theory and Experiment* **2020**, 063204 (2020).
- [24] L. Angelani, R. Di Leonardo, and M. Paoluzzi, First-passage time of run-and-tumble particles, *The European Physical Journal E* **37**, 59 (2014).
- [25] A. Dhar, A. Kundu, S. N. Majumdar, S. Sabhapandit, and G. Schehr, Run-and-tumble particle in one-dimensional confining potentials: Steady-state, relaxation, and first-passage properties, *Physical Review E* **99**, 032132 (2019).
- [26] K. Malakar, V. Jemseena, A. Kundu, K. Vijay Kumar, S. Sabhapandit, S. N. Majumdar, S. Redner, and A. Dhar, Steady state, relaxation and first-passage properties of a run-and-tumble particle in one-dimension, *Journal of Statistical Mechanics: Theory and Experiment* **2018**, 043215 (2018).
- [27] M. Guéneau, S. N. Majumdar, and G. Schehr, Optimal mean first-passage time of a run-and-tumble particle in a class of one-dimensional confining potentials, *Europhysics Letters* **145**, 61002 (2024).
- [28] M. Guéneau, S. N. Majumdar, and G. Schehr, Run-and-tumble particle in one-dimensional potentials: Mean first-passage time and applications, *Physical Review E* **111**, 014144 (2025).
- [29] B. De Bruyne, S. N. Majumdar, and G. Schehr, Survival probability of a run-and-tumble particle in the presence of a drift, *Journal of Statistical Mechanics: Theory and Experiment* **2021**, 043211 (2021).
- [30] F. Mori, P. Le Doussal, S. N. Majumdar, and G. Schehr, Universal Survival Probability for a d-Dimensional Run-and-Tumble Particle, *Physical Review Letters* **124**, 090603 (2020).
- [31] J. Elgeti and G. Gompper, Self-propelled rods near surfaces, *Europhysics Letters* **85**, 38002 (2009).
- [32] J. Elgeti and G. Gompper, Wall accumulation of self-propelled spheres, *Europhysics Letters* **101**, 48003 (2013).
- [33] Y. Zhao, Active particles in a tube: A generalized entropy potential approach, *Physical Review Research* **7**, 013015 (2025).
- [34] A. P. Solon, Y. Fily, A. Baskaran, M. E. Cates, Y. Kafri, M. Kardar, and J. Tailleur, Pressure is not a state function for generic active fluids, *Nature Physics* **11**, 673 (2015).
- [35] F. Smallenburg and H. Löwen, Swim pressure on walls with curves and corners, *Physical Review E* **92**, 032304 (2015).
- [36] A. Duzgun, Active Brownian particles near straight or curved walls: Pressure and boundary layers, *Physical Review E* **97**, 032606 (2018).
- [37] D. Siegmund, The Equivalence of Absorbing and Reflecting Barrier Problems for Stochastically Monotone Markov Processes, *The Annals of Probability* **4**, 914 (1976).
- [38] M. Guéneau and L. Touzo, Siegmund duality for physicists: A bridge between spatial and first-passage properties of continuous- and discrete-time stochastic processes, *Journal of Statistical Mechanics: Theory and Experiment* **2024**, 083208 (2024).
- [39] P. Lévy, *Processus stochastiques et mouvement brownien*, 2nd ed., Les grands classiques Gauthier-Villars (Ed. J. Gabay, Sceaux, 1992).
- [40] D. V. Lindley, The theory of queues with a single server, *Mathematical Proceedings of the Cambridge Philosophical Society* **48**, 277 (1952).

- [41] J. Cox and U. Rösler, A duality relation for entrance and exit laws for Markov processes, *Stochastic Processes and their Applications* **16**, 141 (1984).
- [42] S. Jansen and N. Kurt, On the notion(s) of duality for Markov processes, *Probability Surveys* **11**, 10.1214/12-PS206 (2014).
- [43] C. Monthus, Markov dualities via the spectral decompositions of the two Markov generators in their bi-orthogonal basis of right and left eigenvectors, *Journal of Statistical Mechanics: Theory and Experiment* **2025**, 103201 (2025).
- [44] M. Guéneau and L. Touzo, Relating absorbing and hard wall boundary conditions for a one-dimensional run-and-tumble particle, *Journal of Physics A: Mathematical and Theoretical* **57**, 225005 (2024).
- [45] M. Guéneau, *Non-Equilibrium Dynamics and First-Passage Properties of Stochastic Processes : From Brownian Motion to Active Particles*, Ph.d. thesis, Sorbonne Université (2025).
- [46] L. Touzo, Exact results for active particle models: from long-range interactions to first-passage properties, [arXiv:2507.17504](https://arxiv.org/abs/2507.17504) (2025).
- [47] Rothschild, Non-random Distribution of Bull Spermatozoa in a Drop of Sperm Suspension, *Nature* **198**, 1221 (1963).
- [48] H. Winet, G. S. Bernstein, and J. Head, Observations on the response of human spermatozoa to gravity, boundaries and fluid shear, *Reproduction* **70**, 511 (1984).
- [49] A. P. Berke, L. Turner, H. C. Berg, and E. Lauga, Hydrodynamic Attraction of Swimming Microorganisms by Surfaces, *Physical Review Letters* **101**, 038102 (2008).
- [50] More generally, even when $p_{\text{eq}}(\vartheta)$ is not constant, the same step goes through provided the ϑ -dynamics is reversible (i.e., satisfies detailed balance) with respect to p_{eq} . One then again obtains (9) without additional ϑ -derivative terms (see Ref. [38]).
- [51] S. Redner, *A Guide to First-Passage Processes* (Cambridge University Press, Cambridge, UK ; New York, 2001).
- [52] J. Klinger, R. Voituriez, and O. Bénichou, Splitting Probabilities of Symmetric Jump Processes, *Physical Review Letters* **129**, 140603 (2022).
- [53] S. N. Majumdar, A. Rosso, and A. Zoia, Hitting Probability for Anomalous Diffusion Processes, *Physical Review Letters* **104**, 020602 (2010).
- [54] M. E. Cates and J. Tailleur, When are active brownian particles and run-and-tumble particles equivalent? consequences for motility-induced phase separation, *Europhysics Letters* **101**, 20010 (2013).
- [55] C. Kurzthaler, Y. Zhao, N. Zhou, J. Schwarz-Linek, C. Devailly, J. Arlt, J.-D. Huang, W. C. K. Poon, T. Franosch, J. Tailleur, and V. A. Martinez, Characterization and control of the run-and-tumble dynamics of *Escherichia coli*, *Physical Review Letters* **132**, 038302 (2024).
- [56] M. Guéneau, S. N. Majumdar, and G. Schehr, Exact Stationary State of a d -dimensional Run-and-Tumble Particle in a Harmonic Potential, [preprint arXiv:2602.08436](https://arxiv.org/abs/2602.08436) (2026).
- [57] D. Frydel, Run-and-tumble particles in slit geometry as a splitting probability problem, *Physics of Fluids* **36**, 111901 (2024).
- [58] M. R. Evans and S. N. Majumdar, Diffusion with stochastic resetting, *Physical Review Letters* **106**, 160601 (2011).
- [59] M. R. Evans, S. N. Majumdar, and G. Schehr, Stochastic resetting and applications, *Journal of Physics A: Mathematical and Theoretical* **53**, 193001 (2020).
- [60] Y. Baouche and C. Kurzthaler, Optimal first-passage times of active brownian particles under stochastic resetting, *Soft Matter* **21**, 5998–6011 (2025).
- [61] V. Kumar, O. Sadekar, and U. Basu, Active Brownian motion in two dimensions under stochastic resetting, *Physical Review E* **102**, 052129 (2020).
- [62] N. Levernier, M. Dolgushev, O. Bénichou, R. Voituriez, and T. Guérin, Survival probability of stochastic processes beyond persistence exponents, *Nature Communications* **10**, 2990 (2019).
- [63] T. Arnoulx De Pirey, From an exact solution of dynamics in the vicinity of hard walls to extreme-value statistics of non-Markovian processes, *Physical Review E* **110**, L062105 (2024).
- [64] P. Malgaretti and H. Stark, Model microswimmers in channels with varying cross section, *The Journal of Chemical Physics* **146**, 174901 (2017).
- [65] O. Granek, Y. Kafri, M. Kardar, S. Ro, J. Tailleur, and A. Solon, Colloquium: Inclusions, boundaries, and disorder in scalar active matter, *Reviews of Modern Physics* **96**, 031003 (2024).
- [66] R. D. Schumm and P. C. Bressloff, Search processes with stochastic resetting and partially absorbing targets, *Journal of Physics A: Mathematical and Theoretical* **54**, 404004 (2021).
- [67] P. C. Bressloff, Trapping of an active Brownian particle at a partially absorbing wall, *Proceedings of the Royal Society A: Mathematical, Physical and Engineering Sciences* **479**, 20230086 (2023).
- [68] P. C. Bressloff, Run-and-tumble particle with diffusion: boundary local times and the zero-diffusion limit, *Journal of Statistical Mechanics: Theory and Experiment* **2025**, 113201 (2025).
- [69] The file is available on [Zenodo](https://zenodo.org/doi/10.5281/zenodo.18982482) (DOI: 10.5281/zenodo.18982482).

End Matter

Perturbation expansion.— The probability density of an ABP between absorbing walls $P_A(z, \vartheta, t|z_0, \vartheta_0)$ satisfies the FPE

$$\partial_t P_A = \mathcal{L}_{z, \vartheta} P_A =: [\mathcal{H}_0 + \text{Pe}\mathcal{V}] P_A, \quad (19)$$

where $\mathcal{H}_0 = D\partial_z^2 + D_{\text{rot}}\partial_\vartheta^2$ and $\mathcal{V} = -(D/L)\cos\vartheta\partial_z$. Transforming to Laplace space ($t \rightarrow s$) and inserting the expansion $P_A = P_A^{(0)} + \text{Pe} P_A^{(1)} + \text{Pe}^2 P_A^{(2)} + \dots$ yields the set of coupled equations

$$(s - \mathcal{H}_0)\widehat{P}_A^{(0)} = \delta(z - z_0)\delta(\vartheta - \vartheta_0), \quad (20a)$$

$$(s - \mathcal{H}_0)\widehat{P}_A^{(i+1)} = \mathcal{V}\widehat{P}_A^{(i)}, \quad i \geq 0, \quad (20b)$$

where the zeroth order $P_A^{(0)}$ corresponds to the propagator of a passive particle with rotational diffusion between two absorbing walls. It is possible to perform an

eigenfunction expansion of the unperturbed FPE and to obtain the Green's function of the unbounded problem:

$$G^u(s, z, \vartheta, z', \vartheta') = \frac{1}{2\pi} \sum_{\ell=-\infty}^{\infty} \frac{1}{2Dp_\ell} e^{-p_\ell|z-z'|} e^{i\ell(\vartheta'-\vartheta)}, \quad (21)$$

where $p_\ell^2 = (s + D_{\text{rot}}\ell^2)/D$. The absorbing boundaries at $z = 0$ and $z = L$ are then enforced by the method of reflections, which gives

$$\widehat{P}_A^{(0)}(z, \vartheta, s | z', \vartheta') = \frac{1}{2\pi} \sum_{\ell=-\infty}^{\infty} e^{i\ell(\vartheta'-\vartheta)} \frac{1}{Dp_\ell \sinh(p_\ell L)} \begin{cases} \sinh(p_\ell z) \sinh(p_\ell(L-z')), & z < z', \\ \sinh(p_\ell z') \sinh(p_\ell(L-z)), & z > z'. \end{cases} \quad (22)$$

Equations (20a) and (20b) lead to the iterative integral relation in Eq. (15), which we use to compute each order of the perturbative expansion. Note that this method is adapted from Ref. [16], where the case of a single absorbing wall was studied.

The explicit corrections to the propagator are lengthy and are not reported here (see the Mathematica Script [69]). Instead, we only quote the first corrections to the main observables.

For the mean first-passage time, we obtain

$$\frac{\langle T(z_0, \vartheta_0) \rangle}{\tau} = \frac{z_0(1-z_0/L)}{2L} + \cos \vartheta_0 \frac{\sinh(\sqrt{\gamma}(z_0/L - \frac{1}{2})) - 2(z_0/L - \frac{1}{2}) \sinh(\frac{1}{2}\sqrt{\gamma})}{2\gamma \sinh(\frac{1}{2}\sqrt{\gamma})} \text{Pe} + O(\text{Pe}^2), \quad (23)$$

with $\gamma = L^2 D_{\text{rot}}/D$. The splitting probability with fixed initial orientation reads

$$\pi_L(z_0, \vartheta_0) = \frac{z_0}{L} + \cos \vartheta_0 \frac{\cosh(\frac{1}{2}\sqrt{\gamma}) - \cosh(\sqrt{\gamma}(z_0/L - \frac{1}{2}))}{\gamma \cosh(\frac{1}{2}\sqrt{\gamma})} \text{Pe} + O(\text{Pe}^2). \quad (24)$$

Finally, averaging over the initial orientation, we find

$$\pi_L(z_0) = \frac{1}{2\pi} \int_0^{2\pi} d\vartheta_0 \pi_L(z_0, \vartheta_0) = \frac{z_0}{L} + \frac{\sinh(\sqrt{\gamma}(z_0/L - \frac{1}{2})) - 2(z_0/L - \frac{1}{2}) \sinh(\frac{1}{2}\sqrt{\gamma})}{2\gamma^{3/2} \cosh(\frac{1}{2}\sqrt{\gamma})} \text{Pe}^2 + O(\text{Pe}^4). \quad (25)$$

Consequences of Siegmund duality.— From the Siegmund identity [Eq. (10)], one can relate first-passage observables of the dynamics with absorbing walls to spatial properties of the dual dynamics with hard walls. Although illustrated here for ABPs, these relations hold for any pair of Siegmund-dual processes and are therefore very general.

First, the survival probability of the ABP in the presence of two absorbing walls at $z = 0$ and $z = L$ is by definition given by

$$S(z_0, t) = \mathbb{P}_A(0 < z(t) < L | z_0), \quad (26a)$$

$$= 1 - \mathbb{P}_A(z(t) = 0 | z_0) - \mathbb{P}_A(z(t) = L | z_0), \quad (26b)$$

$$= \mathbb{P}_A(z(t) \geq 0^+ | z_0) - \mathbb{P}_A(z(t) \geq L | z_0), \quad (26c)$$

where, in the last equality, we used the presence of an absorbing wall at L and that $1 - \mathbb{P}_A(z(t) = 0 | z_0) = \mathbb{P}_A(z(t) \geq 0^+ | z_0)$. Using the Siegmund duality

[Eq. (10)], it follows that

$$S(z_0, t) = \mathbb{P}_H(z(t) \leq z_0 | 0^+) - \mathbb{P}_H(z(t) \leq z_0 | L), \quad (27)$$

yielding Eq. (11) of the main text. In particular, in the presence of one wall (i.e., when $L \rightarrow \infty$), we find

$$S(z_0, t) = \int_0^{z_0} dz p_H(z, t | 0). \quad (28)$$

Hence, the survival probability of a particle initially at z_0 with an absorbing boundary at the origin can be interpreted as the probability that a dual particle, started at the origin and evolving in the presence of a hard wall at the origin, is located in the interval $[0, z_0]$ at time t .

Another important quantity is the MFPT, which follows directly from the survival probability,

$$\langle T \rangle = \int_0^\infty dt S(z_0, t). \quad (29)$$

Using Eq. (11) leads straightforwardly to Eq. (12). The MFPT to either absorbing wall for a particle starting at z_0 can thus be interpreted as the difference between the expected local times accumulated in the interval $[0, z_0]$ by the dual hard-wall dynamics when initialized at 0 and L .

Finally, setting $\tilde{z}_0 = L$ in Eq. (10) relates the exit probability at wall L , defined in Eq. (14) for a particle starting at z_0 , to the probability that the dual hard-wall dynamics lies in $[0, z_0]$ [38],

$$E_L(z_0, t) = \int_0^{z_0} dz p_H(z, t | L). \quad (30)$$

In the long-time limit $t \rightarrow \infty$, the initial condition is forgotten. Taking a derivative with respect to z_0 then yields a direct relation between the splitting probability and the

stationary distribution of the hard-wall dynamics [38],

$$p_H(z) = \frac{\partial \pi_L(z)}{\partial z}, \quad (31)$$

where $\pi_L(z) = \lim_{t \rightarrow \infty} E_L(z, t)$.

Computer simulations.— To corroborate our analytical results, we simulate the equations of motion [Eq. (2)] employing the Euler-Maruyama scheme:

$$\mathbf{r}(t + \Delta t) = \mathbf{r}(t) + \mathbf{v}\mathbf{e}(t)\Delta t + \sqrt{2D\Delta t}\mathbf{N}_\eta, \quad (32a)$$

$$\vartheta(t + \Delta t) = \vartheta(t) + \sqrt{2D_{\text{rot}}\Delta t}N_\xi, \quad (32b)$$

where $\mathbf{N}_\eta(0, 1)$ and $N_\xi(0, 1)$ are independent standard normal random variables with zero mean and unit variance and the time step is set to $\Delta t = 10^{-8}\tau$ when studying the absorbing walls and $\Delta t = 10^{-4}\tau$ when considering hard walls. We simulate 2×10^5 trajectories to obtain reliable statistics.